ACS APPLIED MATERIALS & INTERFACES

Research Article

www.acsami.org

Multiscale Modeling of the Electrostatic Impact of Self-Assembled Monolayers used as Gate Dielectric Treatment in Organic Thin-Film Transistors

Alexander Mityashin,[†,‡] Otello Maria Roscioni,[§] Luca Muccioli,[*,§] Claudio Zannoni,[§] Victor Geskin,[⊥] Jérôme Cornil,[⊥] Dimitri Janssen,[†,#,∥] Soeren Steudel,[†] Jan Genoe,[†] and Paul Heremans[†,‡]

[†]Large Area Electronics, Imec, Kapeldreef 75, Leuven 3001, Belgium

[‡]ESAT, Katholieke Universiteit Leuven, Kasteelpark Arenberg 10, Leuven 3001, Belgium

[§]Department of Industrial Chemistry "Toso Montanari" & INSTM, University of Bologna, Viale del Risorgimento 4, Bologna 40136, Italy

[⊥]Laboratory for Chemistry of Novel Materials, University of Mons, Place du Parc 20, Mons 7000, Belgium

[#]Department of Chemistry, Katholieke Universiteit Leuven, Celestijnenlaan 200F, Leuven 3001, Belgium

Supporting Information

ABSTRACT: This study sheds light on the microscopic mechanisms by which self-assembled monolayers (SAMs) determine the onset voltage in organic thin-film transistors (OTFTs). Experiments and modeling are combined to investigate the self-assembly and electrostatic interaction processes in prototypical OTFT structures (SiO_2/SAM/pentacene), where alkylated and fluoroalkylated silane SAMs are compared. The results highlight the coverage-dependent impact of the SAM on the density of semiconductor states and enable the rationalization and the control of the OTFT characteristics.

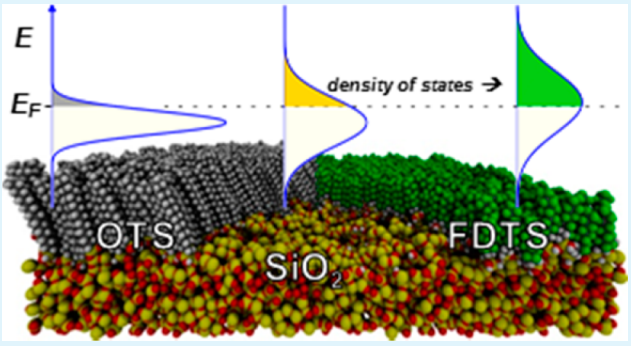

KEYWORDS: *pentacene, electrostatic disorder, onset voltage, molecular dynamics, microelectrostatic model, coverage*

INTRODUCTION

Self-assembled monolayers (SAMs) used as gate dielectric surface treatments in organic thin-film transistors (OTFT) are often believed to be an integral ingredient of a high-performance device.[1] In contact with the semiconducting channel, such treatments can achieve one or more of the following important functions: (i) minimize defects at the dielectric−semiconductor interface; (ii) increase charge carrier mobility; (iii) modulate charge carrier density in the channel; (iv) limit current leakages in thin dielectrics; and (v), and shift the onset voltage (compared to control devices without SAM).[1−5] In inorganic semiconductor technology, these functions are realized by controlled doping. However, doping cannot be used to the same level of control and precision in organic semiconductor technology. In particular, because of the fundamentally different doping mechanism, doping is not active below the part-per-thousand level in organics.[6] Therefore, using SAMs to control the charge density precisely and selectively within the channel is an attractive technological solution.

Despite this concept being routinely used nowadays, the most efficient dielectric-SAM/semiconductor combinations are usually chosen empirically. As such, no consensus has been reached about the actual physical relation between the SAM treatment and OTFT performance. Part of the reason is that, although details of the growth of semiconductors on SAMs have been intensely investigated by various probe techniques and are now relatively easy to control,[7] knowledge of the electronic processes at the SAM/semiconductor interface is scarce. Their understanding is particularly challenging because these processes depend on the subnanometer structure of the interface and thus lie at the limit of spatial resolution of common experimental techniques.

Several concurring theories were suggested to rationalize the experimental observation of high threshold voltage shift and mobility changes: (i) structural changes and general reduction of the spatial roughness in the semiconductor when grown on a SAM; (ii) electronic impact of the SAM end-groups (often depicted as built-in molecular dipoles) inducing charge accumulation or depletion in the adjacent semiconductor; (iii) charge donation from the SAM molecules to the channel, or conversely, charge trapping.[8−12] To clarify these issues, we present in the following a multiscale modeling study of the

Received: June 18, 2014
Accepted: August 14, 2014
Published: August 14, 2014

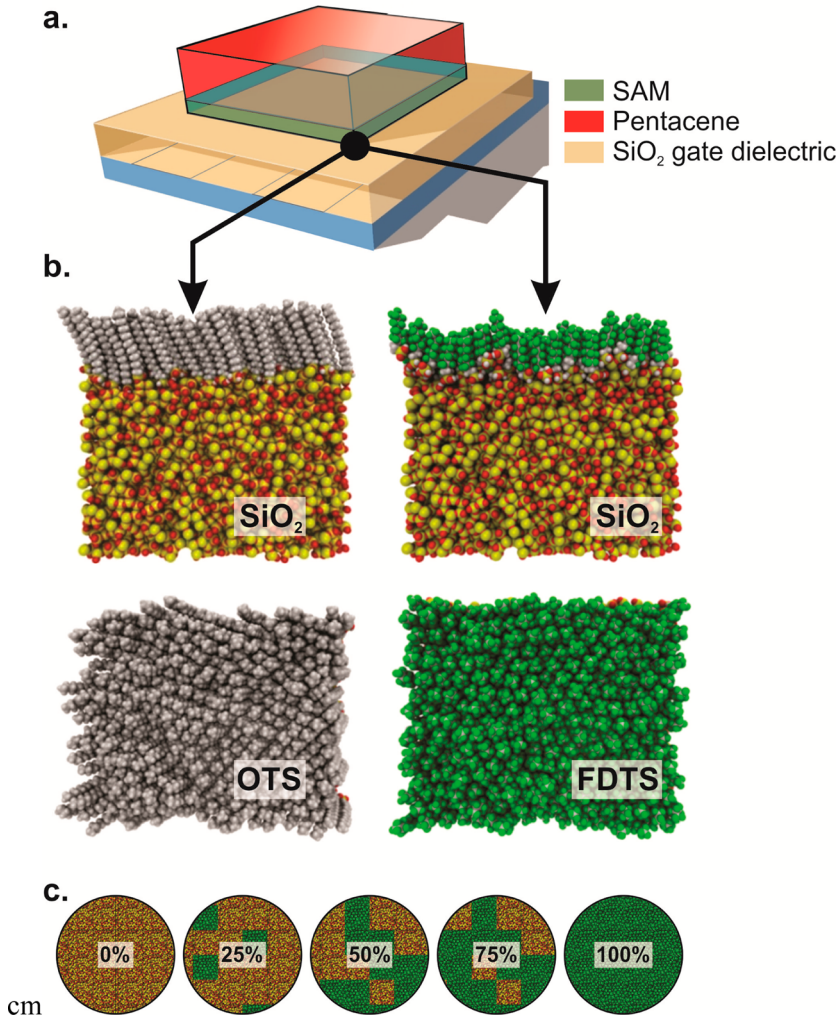

Figure 1. (a) Schematic structure of the studied pentacene-based bottom-gate OTFT device; (b) molecular arrangement of fully covered dielectric-SAM interfaces as obtained by molecular dynamics simulations of the SAM growth on the gate dielectric surface (SiO_2, surface area of the periodic model is 89.8 × 74.9 Å^2). The number of SAM molecules is 302 for OTS, and 256 for FDTS; (c) supercell models with different FDTS coverage envisaged by tiling the bare SiO_2 and SAM-treated samples to mimic the formation of patches due to uncontrolled partial coverage.

structural and electronic properties at dielectric−SAM−semiconductor interfaces.

RESULTS AND DISCUSSION

Our modeling approach comprises four methodologies ranging from micro- to macroscales: density functional theory (DFT), molecular dynamics (MD), microelectrostatics (ME), and macroscale semiconductor modeling. We unravel the effects of SAMs on the density of states in the semiconductor and its impact on the resulting OTFT characteristics; we further complement and support the theoretical results with the experimental characterization of surface coverage and device characteristics of prototypical unipolar SiO_2−SAM-pentacene transistors (see Figure 1a). We chose a very popular chemical family of SAM-forming molecules based on trichlorosilane reactants (R-$SiCl_3$).[13] The condition for obtaining smooth films is believed to be that in which each R-$SiCl_3$ unit forms only a single Si−O− bond with silica, whereas the other two chlorines are replaced by hydroxyl groups upon hydrolysis.[14] In the simulation, we have then opted for the most chemically homogeneous and simple system, studying R-Si-$(OH)_3$ trihydroxyl SAMs in gas phase, and monolayers of monodentate R-Si$(OH)_2$- on SiO_2, where R is either an octadecyl group (OTS SAM) or a 1H,1H′,2H,2H′-perfluorodecyl group (FDTS SAM).

At the smallest spatial scale, density functional theory (DFT) is used to obtain the equilibrium geometry and the HOMO/LUMO levels of individual SAM-forming and organic semiconductor molecules (Table 1). The HOMO/LUMO levels dictate the energy barriers for the charge exchange between SAM and semiconductor and are used to examine the associated charge donation and trapping probabilities. DFT-derived atomic charges are also injected in the molecular dynamics (MD) simulations to parametrize the electrostatic interactions in the force field. During the equilibration stage of MD (∼100 ns), the SAM molecules self-assemble on an ultraflat SiO_2 surface, modeled with a well-validated force field specific for clays (roughness = 2.4 Å, atomic charge on silicon q_{Si} = 2.1 e; atomic charge on oxygen q_O = −1.05 e).[15]

Tightly packed, almost defect-free SAMs (Figure 1b) were obtained by MD simulations in which the molecules were not covalently bonded to the SiO_2 surface, allowing for their migration to the optimal positions through thermal motion,[16] upon equilibration at 300 K. An optimal packing of 4.5 and 3.8 molecules/nm^2 for OTS and FDTS, respectively, was estimated

Table 1. Calculated Gas-Phase HOMO and LUMO Levels of SAM Forming Molecules and Pentacene, Evaluated at Their Equilibrium Geometry with the wB97XD Functional[41] and the cc-pVTZ Basis Set[a]

molecule	HOMO (eV)	LUMO (eV)
pentacene	6.51	1.06
FDTS (R = 1H,1H,2H,2H perfluorodecyl)	10.61	1.80
OTS (R = octadecyl)	9.71	2.55
BUTS (R = 11-bromoundecyl)	9.60	1.99
CUTS (R = 11-cyanoundecyl)	9.88	2.52
PTS (R = phenyl)	8.59	1.70
UETS (R = 10-undecenyl)	9.14	2.39

[a]To maximize the similarity with the chemical structure of SAMs experimentally deposited on SiO_2, we carried out calculations for R-tri-hydroxyl-silanes instead of their R-trichloro-silane precursors. Notice that a possible error of maximum 1 eV is expected when using density functional theory for estimating the band gap of medium-size organic molecules.[42].

from the SAM crystal cell obtained from spontaneous aggregates observed in previous simulations at partial coverage; this range is consistent with experimental and simulated values for OTS,[17,18] whereas we are not aware of similar studies for FDTS. Both SAMs possess a locally crystalline structure characterized by a hexagonal lattice with short-range spatial correlation (see Figure 1b), although OTS is more ordered than FDTS (orientational order parameter P_2 = 0.97 vs 0.86, see the Supporting Information) and tilted (the tilt angle distribution peaks at 23°, in agreement with the experimental range);[14] FDTS molecules are instead standing with their long axis on average normal to the oxide surface.

Larger surfaces at different SAM coverage, ranging from the bare to fully covered oxide, are then constructed by tiling bare SiO_2 and SAM-covered surface elements in a desired proportion (Figure 1c). In our modeling, the coverage percentage has then the physical meaning of the fraction of bare versus SAM-covered surface patches, and should not be confused with a measure of the number of SAM molecules per area for a uniformly covered surface, for example, in experimental studies of Langmuir–Blodgett films.[17] The atomic charge distributions obtained from the generated morphologies are then injected into microelectrostatic (ME) calculations. A mesoscale semiconducting channel, represented by a three-dimensional pentacene crystal (135 molecules) is then placed onto the SiO_2–SAM substrates obtained from the MD simulations. The charge transport landscape in the channel is accessed using the ME model of pentacene developed in a previous study.[19] In this model, a vacancy is moved from one pentacene molecule to another to probe the charge-surface electrostatic interaction E_s as seen by holes during the device operation.

Five monolayers of pentacene arranged in a cylindrical aggregate with a radius of R = 25 Å in the structure of the Siegrist polymorph[20] were placed onto the dielectric-SAM substrate with a spacing of 2 Å. Electrostatically, each pentacene molecule is represented by five chargeable points in the centers of its aromatic rings. A standard vision of full charge localization was adopted.[21] Therefore, to charge the molecule with a hole, a positive charge is equally divided over these five points. The energies of the individual charges are defined by the interactions with their molecular environment. To focus on the effects of the surface, electrostatic interactions between a charge (q_j) in pentacene and the surface charges (q_i) extracted from the MD simulations were calculated on every molecule in the center of the pentacene aggregate (molecules within a cylinder with R = 15 Å) assuming an electrical permittivity ε = 4 typical of organic materials to account for polarization effects:

$$E_s^j = \frac{1}{4\pi\varepsilon r\varepsilon_0}\sum_i \frac{q_j q_i}{r} \quad (1)$$

To address the effects of the SAM coverage, we created quasi-circular surfaces with a radius R = 35 nm from tiles of bare SiO_2 and tiles with a SAM treatment. To define the coverage level, these tiles were randomly intermixed in a desired proportion. To collect a reliable statistics, 1000 random realizations per coverage were constructed and the (local) distribution of E_s was calculated for each surface.

The mean impact of the surface is captured by the spatially averaged value of E_s, which is responsible for charge accumulation/depletion in the adjacent semiconductor: within the standard convention for p-type devices, hole accumulation at the gate dielectric interface corresponds to $E_s > 0$ (with a negative surface potential). E_s depends linearly on the monolayer coverage (Figure 2a) and is always positive for

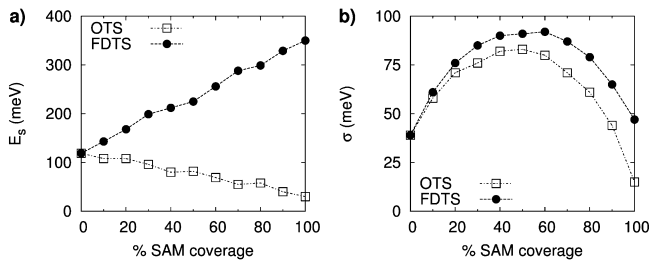

Figure 2. Electrostatic impact of the dielectric surface on the energy level diagram of a thin-film transistor and its dependence on the SAM coverage. (a) Surface-induced electrostatic energy E_s estimated as the spatially averaged charge-surface interaction as a function of the SAM coverage on SiO_2; (b) surface-induced electrostatic disorder σ of pentacene transport levels, captured by the standard deviation of the charge–surface interaction as a function of the SAM coverage on SiO_2.

both SAMs. Compared to the reference SiO_2,($E_s \approx 0.11$ eV, or a potential of −110 mV) fluorinated FDTS increases the hole accumulation (E_s ~0.35 eV or −350 mV at 100% coverage), thus attracting additional charges from the electrodes to the channel, while the effect of OTS is opposite (i.e., decrease of hole accumulation with respect to SiO_2, $E_s \approx 0.03$ eV or −30 mV at 100% coverage) and much less pronounced. These variations of the surface potential are consistent with the considerably higher threshold voltage reported in literature for FDTS transistors with respect to OTS (Table 2). SAMs thus in principle allow for a fine control over the charge accumulation/depletion, which can be exploited to enable complementary circuits using unipolar technology with n-type or p-type behavior defined by the SAM treatment.[22,23]

Another important characteristic is the spatial uniformity of the electrostatic interactions with the surface, captured by its standard deviation σ. The width of the density of states in the organic semiconductor is affected by two main factors: (i) a structural disorder,[24] which is zero for ideal crystalline semiconductors and realistically in a range between 10 and 100 meV,[25] and (ii) an electrostatic contribution induced by the dielectric, here SiO_2 or SiO_2/SAM, depicted in Figure 2b.

Table 2. Experimental Results for Onset (Threshold) Voltages and Hole Mobility for SiO_2/SAM/Pentacene Bottom-Gate Field Effect Transistors

SAM	V_{on} (V_{th}) (V)	mobility ($cm^2/(V\ s)$)	ref
OTS	+4.7 (−3.7)	0.96	32
OTS	(−19)	0.6	17
OTS	(+9.5)	0.52	7
OTS		0.5 ± 0.15	24
OTS	+10	0.517 ± 0.015	this work
octyl-TS	(+5)	0.13	9
FTDS	(+17)	0.2	9
FDTS	+24	0.449 ± 0.002	this work
F-hexyl-TS	+44 (+26)	0.36	32
untreated SiO_2	(−11)	0.086	9
untreated SiO_2	(−10:-4)	0.0075:0.17	43

We found that atomically flat SiO_2, as well as SAMs at high coverage, are fairly uniform and thus introduce only a small electrostatic disorder σ (σ_{SiO2} = 39 meV, σ_{OTS} = 15 meV, σ_{FDTS} = 47 meV). In contrast, electronically and spatially inhomogeneous surfaces at partial coverage induce a significant electronic disorder in the adjacent semiconductor. These variations of the electrostatic potential, albeit small, may yield a significant decrease in the mobility compared to the bare and fully covered surfaces or when switching from a given SAM to another (vide infra); for instance, in ref 26, it was shown theoretically that the hole mobility in the first pentacene monolayer decreases by about 1 order of magnitude when changing the dielectric from weakly polar polystyrene (σ_{PS} = 33 meV) to strongly polar polymethylmetacrylate (σ_{PMMA} = 71 meV).

The calculated charged pentacene-substrate energies are then used to estimate the macroscale device performance. As it is known that the charge transport occurs mainly in the first monolayer,[27] we focus only on the charge carrier concentration there. We derive the charge density (per unit area) in the semiconducting channel and the onset voltage as a function of the SAM treatment and its coverage. By definition, the onset or switch-on voltage V_{on}, the gate voltage that has to be applied to reach the flat band condition,[28] corresponds to the situation of mobile interface charges N_i in the semiconductor exactly matching the charges accumulated at the gate electrode C_gV_{on} and those trapped in the dielectric N_t

$$V_{on} = \frac{N_i - N_t}{C_g} \tag{2}$$

where $C_g = \varepsilon_r\varepsilon_0/d$ is the gate dielectric capacitance per unit area, d the thickness of the dielectric layer, ε_r its relative permittivity, and the charge densities are expressed per unit area as well.[29] Clearly, N_i depends on the intrinsic doping level of the semiconductor—hence, on its chemical nature—but also on the electrostatic potential of the dielectric surface, which is modified by the SAM.[12,22] It follows from eq 2 that the onset voltage can be varied in three distinct and fundamentally different ways

Increasing C_g. The additional SAM capacitance is connected in series with that of the gate dielectric. Since the contribution of the nanometer-thick capacitance is negligible compared to that of typical gate dielectrics, this effect can be neglected in all cases except when nanodielectrics are used.[11,30,31] Here we assumed the typical dielectric capacitance for standard SiO_2 wafer (C_g = 28 nF cm^{-2} for a 120 nm thick SiO_2 dielectric).

Changing N_t. N_t represents the surface density of immobile charges trapped in the dielectric. Typically for SiO_2 this number is not negligible and positive, and it is the origin of the negative onset voltages often measured in SiO_2/pentacene OTFTs.[32] In fact, for a p-type semiconductor, N_i can assume only positive values; therefore, following eq 2, N_t is the only possible source of negative onset voltages. Additional traps may in principle arise at the dielectric-semiconductor interface upon SAM deposition. The trapping probability is defined by the energy offset between the ionization potential of the pentacene semiconductor ($HOMO_{pen}$) and SAM ($HOMO_{SAM}$), $P_t = \exp((HOMO_{SAM} - HOMO_{pen})/kT)$. Note that for hole energy levels, we use here a standard notation with positive values instead of negative ones (cf. also Figure S4 in the Supporting Information). Given that creating a hole in the SAM costs about 2−4 eV more energy than in pentacene (Table 1), the charge trapping probability is also very low and the hole trapping on the SAM molecules correspondingly extremely unlikely- hence we used $N_t^{SAM} = 0$ in all the calculations. It is, however, possible that N_t increases after operating the transistor at high voltages as suggested by recent measurements on the dielectric surface of SAM-decorated SiO_2[12] and polymers.[33] These experiments showed that the electrostatic potential of surfaces exposed to air increases by an order of magnitude after charging, going from hundreds of mV (i.e., in the range predicted by our modeling) to a few volts. Such postoperation effects, whose origin and relation with device properties is still matter of investigation, are outside the scope of the present paper and are not considered in the present model. These charge accumulation electrostatic effects are expected to add up to the electrostatic impact of the SAM discussed here.

Changing N_i. The variation observed in the semiconductor charge density when interfacing the SAM can be ascribed to two main effects: spontaneous charge donation from the SAM to the semiconductor and electrostatic impact of the SAM. To assess the first scenario, the HOMO and LUMO levels of pentacene and typical SAM molecules are compared (Table 1). In all cases, there is a large mismatch between the hole donating levels of the SAMs (i.e., $HOMO_{SAM}$) and the pentacene $LUMO_{pen}$, indicating that SAM molecules cannot transfer holes to pentacene. Although polarization effects in the solid-state can shift the energy levels by over 1 eV,[18] the resulting energy barriers for the hole transfer from the SAM remain too high. Therefore, the charge donation probability at room temperature $P_d = \exp((HOMO_{pen} - LUMO_{SAM})/kT)$ is also negligible. Having excluded the charge donation by the SAM, the Fermi level E_f in the pure semiconductor is only defined by its intrinsic doping level. In order to estimate N_i, we assume a Gaussian density of states

$$g(E) = \frac{1}{\sigma\sqrt{2\pi}}\exp\left(-\frac{(E - E_s + E_h)^2}{2\sigma^2}\right) \tag{3}$$

where E_h is the intrinsic hole transport level, which in the case of bare SiO_2 is shifted of 0.42 eV with respect E_F according to recent Kelvin probe force microscopy measurements[34,35]

The corresponding equilibrium charge density per unit area N_i in the first monolayer is dictated by the occupational Fermi−Dirac statistics $f_F(E)$in the distribution of channel states $g(E)$

$$f_F(E) = \frac{1}{1 + \exp\left(-\frac{E + E_f}{kT}\right)} \tag{4}$$

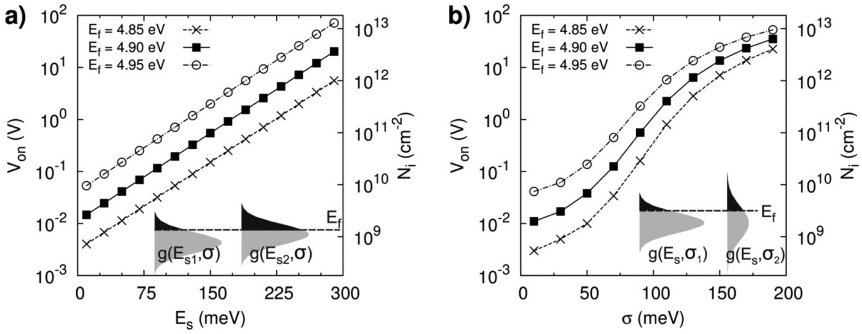

Figure 3. (a) Charge carrier density N_i in the semiconductor channel and onset voltage V_{on} of a thin-film transistor (assuming a 120 nm thick SiO_2 gate dielectric, C_g = 28 nF cm^{-2}, and N_t = 0) as a function of the electrostatic interaction with the surface E_s (with σ = 10 meV). Positive E_s shifts $g(E)$ of the channel states closer to E_f (inset) result in an exponential increase of both N_i and V_{on}. (b) Increasing σ (with E_s = 0) creates new states above E_f (inset), increasing N_i and V_{on}. In both figures, the effect of possible variations of the intrinsic doping concentration is accounted for by plotting the results for three different positions of E_f (4.85, 4.9, 4.95 eV), with E_h fixed to 5.32 eV.

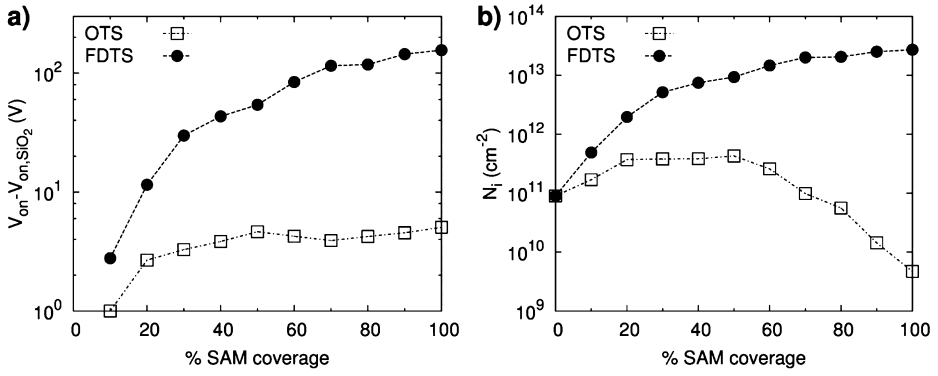

Figure 4. (a) Variation in onset voltages for SiO_2/pentacene/OTS and FDTS SAMs OTFTs as a function of the percentage of the SiO_2 surface covered by the SAM (a), and corresponding charge densities in the channel (b). Values are calculated from eqs 2−5 using the hole-surface electrostatic interaction and standard deviations obtained by theoretical modeling (Figure 2) and assuming E_f = 4.9 eV, E_h = 5.32 eV, $N_t^{SiO_2}$= 9.9 × 10^{11} cm^{-2} (corresponding to an onset voltage of −5 V for for a 120 nm SiO_2 gate dielectric), N_t^{SAM}= 0, and a complete screening of SiO_2 trapped charges by the SAM ($N_t = N_t^{SiO_2}(1 - x)$, where x is the fractional SAM coverage).

$$N_i = N_0\left[\int_{+\infty}^{-\infty} g(E) f_F(E) dE\right]^{2/3} \quad (5)$$

where N_0 is the total density of states equal to the surface density of molecules (we used N_0 = 1 × 10^{14} cm^{-2} for pentacene), and the power of 2/3 is introduced to obtain a surface density.

The impact of the SAM on $g(E)$ and N_i is captured by the average charge-surface interaction E_s and its standard deviation σ in eq 3. If σ is kept constant, positive values of E_s shift the semiconductor energy distribution $g(E)$ closer to the Fermi level E_f, as schematically represented by the larger black areas in the Gaussian distributions in Figure 3a, resulting in an exponential increase of N_i (hole accumulation, Figure 3a, right axis) and V_{on}. In Figure 3b, when instead E_s is kept constant, it can be noticed that increasing σ effectively creates new states above E_f which also results in a higher population of the channel states, although this effect is weaker compared to the quasi-exponential trend seen in Figure 3a, at least for σ <100 meV typical of SAM treatments (c.f. Figure 2b). It is important to note that σ is always positive and can only increase/decrease the population of charge carriers of both signs, while playing with the sign of E_s (e.g., by changing the SAM dipole orientation) promotes selective electron or hole accumulation.[30] With our choice of C_g (28 nFcm^{-2}), the observed increase of N_i corresponds to V_{on} shifts up to 100 V (Figure 3, left axes). This effect is especially apparent in lightly doped materials, where E_f lies far from the center of the density-of-state distribution function $g(E)$. Much lower onset voltage shifts can obviously be achieved by considering higher dielectric constant and ultrathin dielectric substrates.[3,4]

To assess the reliability of the modeling results, FDTS and OTS monolayers were vapor deposited onto solvent-cleaned SiO_2 (120 nm) surfaces; a pentacene film (30 nm) was then evaporated on top of it and finally Au source-drain contacts were applied. The deposition conditions were optimized in order to obtain comparable pentacene growth. Device characteristics on bare SiO_2 were hardly reproducible (and thus not discussed here), most likely due to the hydrophilic nature of SiO_2 leading to adsorbed water at the dielectric−semiconductor interface that favors uncontrollable trapping.[36]

Extracted charge carrier mobilities and onset voltages agree qualitatively with the modeling results and previous experiments (Table 2): a much stronger hole accumulation is expected for FDTS, thus increasing the onset voltage (+24 V versus +10 V for OTS). Taking into account the capacitance C_g, and plugging the measured onset voltages in eq 2 with N_t = 0, N_i is extracted to be 4.3 × 10^{12} cm^{-2} and 1.8 × 10^{12} cm^{-2} for FDTS and OTS, respectively, in good qualitative agreement with literature values.[32] A straightforward comparison with our theoretical modeling is not completely fair, because among the different variables that contribute to determining the onset

voltage (C_g, N_t, E_f, E_h, E_s, and σ), only C_g is exactly known in our measurements. It can be noticed that comparing the experimentally derived charge densities above-reported with the theoretical ones in Figure 4b, say at 100% coverage, the latter appear to overestimate the difference between FDTS and OTS, so the accord is only qualitative.

In general, the quality of the SAM coverage is extremely sensitive to the pretreatment conditions (c.f. total reflection X-ray fluorescence characterization in the Supporting Information),[37] which might explain, together with the different capacitances, the large spread in published device characteristics for those systems (see Table 2). No perfect coverage can be guaranteed by macroscopically averaged measurements of contact angle. Vapor-deposited trichlorosilane SAMs are likely to operate at high but not full coverage, differently from solution-deposited SAM-based field-effect transistors (SAMFETs), where monolayer formation requires several days in solution.[38] Our semiquantitative theoretical analysis shows that SAM coverage is as important as the SAM chemistry for the device performance. For instance, the full surface passivation and zero onset voltage is only possible at close to 100% OTS coverage, and a high variability on the onset voltage is expected if the coverage is incomplete or uncontrolled (Figure 4).

CONCLUSIONS

In summary, we set up a multiscale modeling framework aimed at evaluating the impact of a gate dielectric self-assembled monolayer on the transport levels of an organic semiconductor, and applied it to the comparison between fluorinated (FDTS) and alkylated SAMS (OTS) used in SiO_2/SAM/pentacene unipolar transistors, considering also the effect of the SAM coverage. The first significant effect at surfaces with partial coverage is the surface-induced electronic disorder σ in the adjacent semiconductor (Figure 2b). This disorder broadens the distribution of charge transport states $g(E)$ and consequently: (i) increases the number of charge carriers above the Fermi level, (ii) may reduce or increase the carrier mobility, depending on the nature of the semiconductor[39] and whether the formation of deep traps[26] or the increased charge density prevails; although the prediction of charge carrier mobilities is beyond the reach of our model, the interested reader may exploit the knowledge of $g(E)$ in one of several phenomenological approaches that can be employed to estimate them.[40]

The second effect is due to the electrostatic interaction E_s between the SAM and semiconductor, which rigidly shifts the transport levels of the semiconductor, inducing either hole or electron accumulation according to its sign. For the specific case of OTS and FDTS, we found at full coverage that the latter induces a strong hole accumulation with respect to bare SiO_2 ($E_s \approx 350$ meV vs 110 meV for silica), while OTS in practice does not interact with holes ($E_s \approx 30$ meV).

The two SAMs are also very different from the point of view of the width of the energetic disorder σ: FDTS is very similar to SiO_2 in this respect ($\sigma_{SiO_2} = 39$ meV, $\sigma_{FDTS} = 47$ meV at full coverage), whereas OTS at full coverage smooths the energy landscape for charge carriers ($\sigma_{OTS} = 15$ meV). The onset voltage is a growing function of both the surface-semiconductor interaction E_s and its standard deviation σ. As E_s is typically positive and much larger for FDTS than for OTS, and σ is larger as well, our model predicts values of V_{on} of up to a hundred of volts for FDTS, and on the order of a few volts for OTS, consistently with experimental measurements. Remarkably, the variations of E_s and σ are sufficient to explain the scattering of measured threshold voltages in SiO_2/SAM/pentacene transistors, without the need of postulating the presence of trapped charges within the OTS or FDTS SAMs. More in general, we provided a simple but effective theoretical framework that establishes a clear relationship between the microscopic variables in play (C_g, N_t, E_f, E_h, E_s, and σ) with the density of charges in the channel N_i and the onset voltage V_{on}.

ASSOCIATED CONTENT

Supporting Information

Description of atomistic force field customization and Molecular Dynamics simulation details. Experimental details for device preparation and total reflection X-ray fluorescence characterization of SAM coverage. This material is available free of charge via the Internet at http://pubs.acs.org.

AUTHOR INFORMATION

Corresponding Author

*E-mail: Luca.Muccioli@unibo.it. Phone: +39 051 2093387. Fax: +39 051 2093690.

Present Address

[||]D.J. is currently affiliated with Fujifilm Electronic Materials Europe NV, Zwijndrecht, Belgium.

Notes

The authors declare no competing financial interest.

ACKNOWLEDGMENTS

The research leading to these results has received funding from the European Commission Seventh Framework Programme (FP7/2007-2013) under Grant Agreement 228424 Project MINOTOR. P.H. acknowledges financial support of the European Research Council by Grant 320680 (EPOS CRYSTALLI). J.C. is an FNRS Research Director. D.J. acknowledges the Flemish Government agency IWT for funding his PhD scholarship.

REFERENCES

(1) Di Benedetto, S. A.; Facchetti, A.; Ratner, M. A.; Marks, T. J. Molecular Self-Assembled Monolayers and Multilayers for Organic and Unconventional Inorganic Thin-Film Transistor Applications. *Adv. Mater.* **2009**, *21*, 1407−1433.

(2) Aswal, D. K.; Lenfant, S.; Guerin, D.; Yakhmi, J. V.; Vuillaume, D. Self Assembled Monolayers on Silicon for Molecular Electronics. *Anal. Chim. Acta* **2006**, *568*, 84−108.

(3) Ponce Ortiz, R.; Facchetti, A.; Marks, T. J. High-K Organic, Inorganic, and Hybrid Dielectrics for Low-Voltage Organic Field-Effect Transistors. *Chem. Rev.* **2010**, *110*, 205−239.

(4) Martínez Hardigree, J. F.; Dawidczyk, T. J.; Ireland, R. M.; Johns, G. L.; Jung, B.-J.; Nyman, M.; Osterbacka, R.; Marković, N.; Katz, H. E. Reducing Leakage Currents in N-Channel Organic Field-Effect Transistors Using Molecular Dipole Monolayers on Nanoscale Oxides. *ACS Appl. Mater. Interfaces* **2013**, *5*, 7025−7032.

(5) Ma, H.; Acton, O.; Hutchins, D. O.; Cernetic, N.; Jen, A. K.-Y. Multifunctional Phosphonic Acid Self-Assembled Monolayers on Metal Oxides as Dielectrics, Interface Modification Layers and Semiconductors for Low-Voltage High-Performance Organic Field-Effect Transistors. *Phys. Chem. Chem. Phys.* **2012**, *14*, 14110−14126.

(6) Mityashin, A.; Olivier, Y.; Van Regemorter, T.; Rolin, C.; Verlaak, S.; Martinelli, N. G.; Beljonne, D.; Cornil, J.; Genoe, J.; Heremans, P. Unraveling the Mechanism of Molecular Doping in Organic Semiconductors. *Adv. Mater.* **2012**, *24*, 1535−1539.

(7) Ito, Y.; Virkar, A. A.; Mannsfeld, S.; Oh, J. H.; Toney, M.; Locklin, J.; Bao, Z. Crystalline Ultrasmooth Self-Assembled Monolayers of Alkylsilanes for Organic Field-Effect Transistors. *J. Am. Chem. Soc.* **2009**, *131*, 9396−9404.
(8) Sun, X.; Liu, Y.; Di, C.; Wen, Y.; Guo, Y.; Zhang, L.; Zhao, Y.; Yu, G. Interfacial Heterogeneity of Surface Energy in Organic Field-Effect Transistors. *Adv. Mater.* **2011**, *23*, 1009−1014.
(9) Kobayashi, S.; Nishikawa, T.; Takenobu, T.; Mori, S.; Shimoda, T.; Mitani, T.; Shimotani, H.; Yoshimoto, N.; Ogawa, S.; Iwasa, Y. Control of Carrier Density by Self-Assembled Monolayers in Organic Field-Effect Transistors. *Nat. Mater.* **2004**, *3*, 317−322.
(10) Possanner, S. K.; Zojer, K.; Pacher, P.; Zojer, E.; Schürrer, F. Threshold Voltage Shifts in Organic Thin-Film Transistors Due to Self-Assembled Monolayers at the Dielectric Surface. *Adv. Funct. Mater.* **2009**, *19*, 958−967.
(11) Salinas, M.; Jäger, C. M.; Amin, A. Y.; Dral, P. O.; Meyer-Friedrichsen, T.; Hirsch, A.; Clark, T.; Halik, M. The Relationship between Threshold Voltage and Dipolar Character of Self-Assembled Monolayers in Organic Thin-Film Transistors. *J. Am. Chem. Soc.* **2012**, *134*, 12648−12652.
(12) Gholamrezaie, F.; Andringa, A.-M.; Roelofs, W. S. C.; Neuhold, A.; Kemerink, M.; Blom, P. W. M.; de Leeuw, D. M. Charge Trapping by Self-Assembled Monolayers as the Origin of the Threshold Voltage Shift in Organic Field-Effect Transistors. *Small* **2011**, *8*, 241−245.
(13) Wasserman, S. R.; Tao, Y. T.; Whitesides, G. M. Structure and Reactivity of Alkylsiloxane Monolayers Formed by Reaction of Alkyltrichlorosilanes on Silicon Substrates. *Langmuir* **1989**, *5*, 1074−1087.
(14) Wang, M.; Liechti, K. M.; Wang, Q.; White, J. M. Self-Assembled Silane Monolayers: Fabrication with Nanoscale Uniformity. *Langmuir* **2005**, *21*, 1848−1857.
(15) Wang, J.; Kalinichev, A. G.; Kirkpatrick, R. J.; Cygan, R. T. Structure, Energetics, and Dynamics of Water Adsorbed on the Muscovite (001) Surface: A Molecular Dynamics Simulation. *J. Phys. Chem. B* **2005**, *109*, 15893−15905.
(16) Ahn, Y.; Saha, J. K.; Schatz, G. C.; Jang, J. Molecular Dynamics Study of the Formation of a Self-Assembled Monolayer on Gold. *J. Phys. Chem. C* **2011**, *115*, 10668−10674.
(17) Virkar, A.; Mannsfeld, S.; Oh, J. H.; Toney, M. F.; Tan, Y. H.; Liu, G.; Scott, J. C.; Miller, R.; Bao, Z. The Role of OTS Density on Pentacene and C_{60} Nucleation, Thin Film Growth, and Transistor Performance. *Adv. Funct. Mater.* **2009**, *19*, 1962−1970.
(18) Ewers, B. W.; Batteas, J. D. Molecular Dynamics Simulations of Alkylsilane Monolayers on Silica Nanoasperities: Impact of Surface Curvature on Monolayer Structure and Pathways for Energy Dissipation in Tribological Contacts. *J. Phys. Chem. C* **2012**, *116*, 25165−25177.
(19) Verlaak, S.; Heremans, P. Molecular Microelectrostatic View on Electronic States near Pentacene Grain Boundaries. *Phys. Rev. B* **2007**, *75*, 115127.
(20) Siegrist, T.; Kloc, C.; Schön, J. H.; Batlogg, B.; Haddon, R. C.; Berg, S.; Thomas, G. A. Enhanced Physical Properties in a Pentacene Polymorph. *Angew. Chem., Int. Ed.* **2001**, *40*, 1732−1736.
(21) Capek, E. A.; Silinsh, V. *Organic Molecular Crystals. Interaction, Localization and Transport Phenomena*; AIP Press: New York, 1994.
(22) Huang, C.; Katz, H. E.; West, J. E. Solution-Processed Organic Field-Effect Transistors and Unipolar Inverters Using Self-Assembled Interface Dipoles on Gate Dielectrics. *Langmuir* **2007**, *23*, 13223−13231.
(23) Zschieschang, U.; Ante, F.; Schlörholz, M.; Schmidt, M.; Kern, K.; Klauk, H. Mixed Self-Assembled Monolayer Gate Dielectrics for Continuous Threshold Voltage Control in Organic Transistors and Circuits. *Adv. Mater.* **2010**, *22*, 4489−4493.
(24) Yang, H.; Shin, T. J.; Ling, M.-M.; Cho, K.; Ryu, C. Y.; Bao, Z. Conducting AFM and 2D GIXD Studies on Pentacene Thin Films. *J. Am. Chem. Soc.* **2005**, *127*, 11542−11543.
(25) Structural disorder can be analytically included by calculating the total standard deviation as the square root of the sum of structural and electrostatic disorder variances.
(26) Martinelli, N. G.; Savini, M.; Muccioli, L.; Olivier, Y.; Castet, F.; Zannoni, C.; Beljonne, D.; Cornil, J. Modeling Polymer Dielectric/Pentacene Interfaces: On the Role of Electrostatic Energy Disorder on Charge Carrier Mobility. *Adv. Funct. Mater.* **2009**, *19*, 3254−3261.
(27) Shehu, A.; Quiroga, S. D.; D'Angelo, P.; Albonetti, C.; Borgatti, F.; Murgia, M.; Scorzoni, A.; Stoliar, P.; Biscarini, F. Layered Distribution of Charge Carriers in Organic Thin Film Transistors. *Phys. Rev. Lett.* **2010**, *104*, 246602.
(28) Meijer, E. J.; Tanase, C.; Blom, P. W. M.; van Veenendaal, E.; Huisman, B.-H.; de Leeuw, D. M.; Klapwijk, T. M. Switch-on Voltage in Disordered Organic Field-Effect Transistors. *Appl. Phys. Lett.* **2002**, *80*, 3838.
(29) It is implicitly assumed that the workfunction of the gate is the same as the Fermi level of the semiconductor so that the flat-band voltage is neglected. Although the flat-band voltage can easily be included in the equation, it is usually small, and its neglect allows for a more comprehensive comparison of the effect of different doping densities.
(30) Chung, Y.; Verploegen, E.; Vailionis, A.; Sun, Y.; Nishi, Y.; Murmann, B.; Bao, Z. Controlling Electric Dipoles in Nanodielectrics and Its Applications for Enabling Air-Stable N-Channel Organic Transistors. *Nano Lett.* **2011**, *11*, 1161−1165.
(31) Martínez Hardigree, J. F.; Katz, H. E. Through Thick and Thin: Tuning the Threshold Voltage in Organic Field-Effect Transistors. *Acc. Chem. Res.* **2014**, *47*, 1369−1377.
(32) Pernstich, K. P.; Haas, S.; Oberhoff, D.; Goldmann, C.; Gundlach, D. J.; Batlogg, B.; Rashid, A. N.; Schitter, G. Threshold Voltage Shift in Organic Field Effect Transistors by Dipole Monolayers on the Gate Insulator. *J. Appl. Phys.* **2004**, *96*, 6431.
(33) Dawidczyk, T. J.; Martínez Hardigree, J. F.; Johns, G. L.; Ozgun, R.; Alley, O.; Andreou, A. G.; Markovic, N.; Katz, H. E. Visualizing and Quantifying Charge Distributions Correlated to Threshold Voltage Shifts in Lateral Organic Transistors. *ACS Nano* **2014**, *8*, 2714−2724.
(34) Yogev, S.; Halpern, E.; Matsubara, R.; Nakamura, M.; Rosenwaks, Y. Direct Measurement of Density of States in Pentacene Thin Film Transistors. *Phys. Rev. B* **2011**, *84*, 165124.
(35) Yogev, S.; Matsubara, R.; Nakamura, M.; Zschieschang, U.; Klauk, H.; Rosenwaks, Y. Fermi Level Pinning by Gap States in Organic Semiconductors. *Phys. Rev. Lett.* **2013**, *110*, 036803.
(36) Chua, L.-L.; Zaumseil, J.; Chang, J.-F.; Ou, E. C.-W.; Ho, P. K.-H.; Sirringhaus, H.; Friend, R. H. General Observation of N-Type Field-Effect Behaviour in Organic Semiconductors. *Nature* **2005**, *434*, 194−199.
(37) Lee, W. H.; Cho, J. H.; Cho, K. Control of Mesoscale and Nanoscale Ordering of Organic Semiconductors at the Gate Dielectric/Semiconductor Interface for Organic Transistors. *J. Mater. Chem.* **2010**, *20*, 2549.
(38) Smits, E. C. P.; Mathijssen, S. G. J.; van Hal, P. A.; Setayesh, S.; Geuns, T. C. T.; Mutsaers, K. A. H. A.; Cantatore, E.; Wondergem, H. J.; Werzer, O.; Resel, R.; et al. Bottom-up Organic Integrated Circuits. *Nature* **2008**, *455*, 956−959.
(39) Stassen, A. F.; de Boer, R. W. I.; Iosad, N. N.; Morpurgo, A. F. Influence of the Gate Dielectric on the Mobility of Rubrene Single-Crystal Field-Effect Transistors. *Appl. Phys. Lett.* **2004**, *85*, 3899.
(40) Tessler, N.; Preezant, Y.; Rappaport, N.; Roichman, Y. Charge Transport in Disordered Organic Materials and Its Relevance to Thin-Film Devices: A Tutorial Review. *Adv. Mater.* **2009**, *21*, 2741−2761.
(41) Chai, J.-D.; Head-Gordon, M. Long-Range Corrected Hybrid Density Functionals with Damped Atom-Atom Dispersion Corrections. *Phys. Chem. Chem. Phys.* **2008**, *10*, 6615−6620.
(42) Salzner, U.; Aydin, A. Improved Prediction of Properties of Π-Conjugated Oligomers with Range-Separated Hybrid Density Functionals. *J. Chem. Theory Comput.* **2011**, *7*, 2568−2583.
(43) Suemori, K.; Uemura, S.; Yoshida, M.; Hoshino, S.; Takada, N.; Kodzasa, T.; Kamata, T. Influence of Fine Roughness of Insulator Surface on Threshold Voltage Stability of Organic Field-Effect Transistors. *Appl. Phys. Lett.* **2008**, *93*, 033308.